

Short communication

A kinetic expression for the pyrolytic decomposition of polytetrafluoroethylene

Izak J. van der Walt^a, Hein W.J.P. Neomagus^b, Johann T. Nel^a,
O.S.L. Bruinsma^b, Philippus L. Crouse^{c,*}

^aThe South African Nuclear Energy Corporation Ltd. (NECSA), Church Street Extension, Pelindaba, Pretoria 0216, South Africa

^bSchool of Chemical and Minerals Engineering, North-West University, Hoffman Street, Potchefstroom 2531, South Africa

^cFluoro-materials Science & Process Integration, Department of Chemical Engineering,
University of Pretoria, Lynnwood Road, Pretoria 0002, South Africa

Received 30 November 2007; received in revised form 8 January 2008; accepted 10 January 2008

Available online 18 January 2008

Abstract

Despite the fact that the thermal decomposition of polytetrafluoroethylene has been extensively studied over the past six decades, some inconsistencies regarding the kinetic parameters, *e.g.* the order of the reaction, remain. Representative kinetic data are essential for practical purposes such as reactor design and scaling. In general the literature data refer to homogeneous bulk heating, whereas the case of the non-homogeneous heating of a single particle has not received attention. Data (reaction rate and pre-exponential factor) applicable to this latter case were experimentally determined from isothermal thermogravimetric analyses of the depolymerisation reaction of PTFE. The kinetic data obtained on coarse granules (800–1000 μm) are reported here. The rate law is consistent with a shrinking particle kinetic model, with chemical kinetics controlling phase-boundary movement. The mass loss rate is directly proportional to surface area. A rate law applicable to this case, and useable for geometries of arbitrary shape, is derived.

© 2008 Elsevier B.V. All rights reserved.

Keywords: PTFE; Pyrolysis; Kinetics; Decomposition

1. Introduction

It has long been known that the thermal decomposition of polytetrafluoroethylene (PTFE) predominantly yields tetrafluoroethylene (TFE), hexafluoropropylene (HFP), and octafluorocyclobutane (OFCB) [1]. The product ratios can be tailored by manipulating the working temperature, the pressure, the residence time of the gaseous product stream in the hot zone, and the quench rate [2,3]. PTFE is non-melt-processible, hence one of the recycling methods is *via* pyrolysis of the solid waste and subsequent recovery of the monomer for re-use. For this process solid waste is ground down to coarse granules rather than powder, for economic and practical reasons. Knowledge of depolymerisation kinetics is essential for reactor design and industrial scaling. Despite the fact that work on PTFE depolymerisation has been extensively reported since

shortly after the first discovery of the material, and despite the fact that particle size effects are well known in thermogravimetric analysis (TGA) [4] this group of authors found the available literature data, *e.g.* [5–11] to be inadequate for design purposes and, crucially, not to address sample geometry.

Doyle, for example, in an early paper presenting an integral method for obtaining kinetic parameters from thermogravimetric (TG) data [5] reported results obtained using pulverized PTFE. He regarded the pre-exponential factor as trivial, assumed first-order kinetics (*i.e.* assumed the decomposition to be directly proportional to mass), and reported activation energy as the only meaningful kinetic parameter. Siegle et al., investigating PTFE films, similarly assumed first-order kinetics and reported an Arrhenius expression based on mass only [6]. Cox et al. reported TG results pertaining to a large range of fluoropolymers, including PTFE, again only determining activation energies [7]. Carrol and Manche [8], using a differential technique on a non-disclosed PTFE sample type, reported a discontinuity in the mass-loss data at 520 °C, determined two activation energies without corresponding pre-

* Corresponding author. Tel.: +27 12420 2856; fax: +27 12 420 5048.

E-mail address: philip.crouse@up.ac.za (P.L. Crouse).

exponential factors, with two discrete rates, both displaying zero-order kinetics. Holzknacht reported an analytical solution for evaluating evaporation rates and one-dimensional temperature profiles for PTFE particles passing through a high-temperature plasma [9]. Of importance, however, the ablation rate was not determined in the experimental work; rather historical rate data, based on first-order kinetics, were used. Morisaki focused on the mass spectrometric analysis of the gaseous products formed during PTFE pyrolysis, and only reported an activation energy for the process [10]. More recently Conesa and Font suggested that two solid-state decomposition processes take place in parallel during PTFE thermolysis, fitted two n th-order rate equations to the data, and reported mass-based kinetic parameters for the two processes, without any attempt at rationalizing or interpreting the two reaction orders they reported [11].

All the cases above implicitly attempted to achieve homogenous bulk heating of the sample, with good contact with the sample holder. For industrial cases such as ours [2], where coarse granules are used for depolymerisation and where contact with hot surface areas is expected to be poor, radiative heating is anticipated to contribute significantly to energy transfer. In light of this, and some apparent lack of congruence in the literature, the decision was made to re-evaluate the thermal depolymerisation kinetics of PTFE, of granule size typical of what would be used for commercial depolymerisation. We report the results in this short communication and present, we believe for the first time, a reasonable interpretation of the experimentally determined reaction order for large PTFE granules where non-homogeneous heating is expected, and a rate law in a form usable in practice.

2. Results and discussion

2.1. Isothermal decomposition data

Isothermal TGA mass loss data of 800–1000 μm OD PTFE granules at temperatures ranging from 530 to 620 °C are given in Fig. 1.

Each granule was placed loosely in the sample pan, with the only contact being the bottom of the particle where it touched

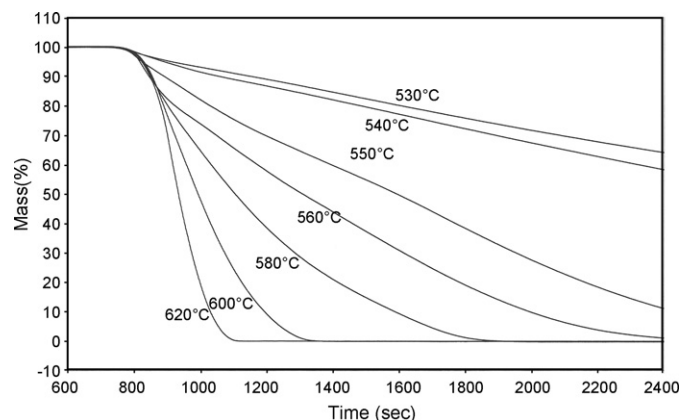


Fig. 1. Isothermal mass loss of unfilled PTFE.

the pan. Heating can thus as a first approximation be assumed to be partially conductive and, because of the low thermal conductivity of the polymer, to have a large radiative component—from the hot surfaces of the sides of the pan and the body of the micro-reactor.

2.2. Empirical kinetic parameters

In order to determine the order of the reaction and rate constant, a rate law of the form

$$-\frac{d\alpha}{dt} = k' \cdot \alpha^n \quad (1)$$

is assumed. Here α is the residual PTFE mass fraction at time t (in s), k' is the depolymerisation rate constant (in s^{-1}), and n is the reaction order. To determine values for k' and n from experimental results, the logarithmic form of Eq. (1), *i.e.*

$$-\ln\left(\frac{d\alpha}{dt}\right) = \ln k' + n \ln \alpha \quad (2)$$

is used. Plots of $\ln(d\alpha/dt)$, versus $\ln \alpha$ thus yield straight lines, the slope of which gives the reaction order, with the rate constant calculated from the y-intercept, as shown in Fig. 2.

Values of n and k' obtained in this way are presented in Table 1.

As is evident from the table, the reaction order does not vary significantly, nor systematically, from temperature to temperature, and an average value of 0.54 is obtained. The Arrhenius plot (*i.e.* a plot of the logarithms of the left-hand and right-hand side of $k' = k'_0 e^{-E_a/RT}$, k'_0 being the pre-exponential factor and E_a the activation energy) using the values given in Table 1 is presented in Fig. 3.

The data in Fig. 3 yield an activation energy equal to 260 kJ mol^{-1} and a pre-exponential factor $k'_0 = 1.78 \times 10^{13} \text{ s}^{-1}$.

2.3. Interpretation of the reaction order

The reaction order we determined seems directly relatable to a phase-boundary controlled process. The average value for the reaction order suggests a particle shape somewhere between a sphere and a cylinder [12]. It seems to be common practice in the TGA literature that the rate constant is quoted as a

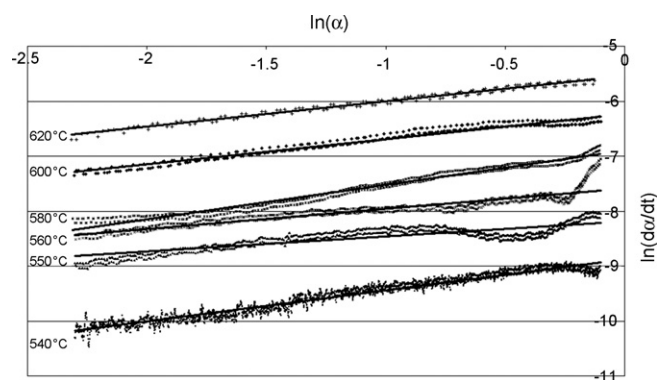


Fig. 2. Graphical determination of reaction order.

Table 1
Order of reaction and rate constants at different temperatures

T (°C)	n	k' (s ⁻¹)
530	0.48	$2.60 \cdot 10^{-4}$
540	0.57	$2.88 \cdot 10^{-4}$
550	0.66	$7.82 \cdot 10^{-4}$
560	0.57	$1.14 \cdot 10^{-3}$
580	0.48	$1.94 \cdot 10^{-3}$
600	0.47	$4.03 \cdot 10^{-3}$
620	0.50	$9.45 \cdot 10^{-3}$
Average	0.54 ± 0.08	–

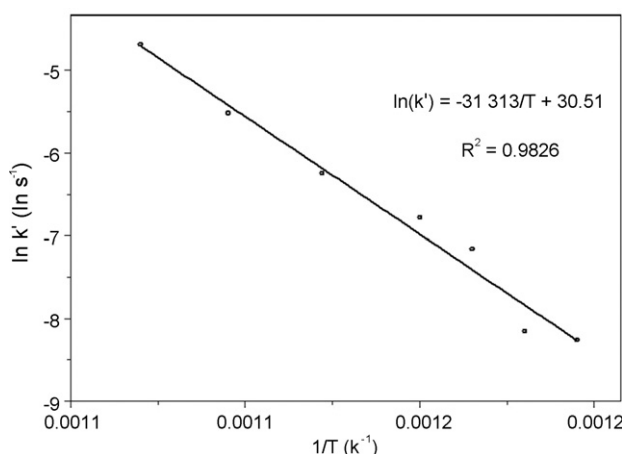


Fig. 3. Arrhenius plot of temperature dependent rate constant.

composite parameter, without including geometry or density [4,12]. In order to tighten the interpretation of the exponent, and to include particle size in the rate, it is useful to examine the derivation of these equations. Consider the sublimation/evaporation of a solid particle, of homogenous material B :



Following the approach taken by, for example, Levenspiel [13], and assuming the sublimation rate to be controlled by and linearly dependent on the available, time-dependent surface $dA(\mathbf{r}(t))$, whose surface contours are described by the position vector $\mathbf{r}(t)$, the generalized sublimation rate becomes

$$-\frac{1}{dA(\mathbf{r}(t))} \frac{dm_{B(s)}}{dt} = k. \quad (4)$$

For the specific case of a sphere, the area is simply $4\pi r^2$, r being the radius. The differential change in particle mass, expressed in terms of radius, is obtained by differentiating the density–volume product, *viz.* $dm_{B(s)} = d(\rho(4/3)\pi r^3) = \rho 4\pi r^2 dr$. Substitution of these values into Eq. (4) yields

$$-\frac{\rho_{B(s)} 4\pi r^2}{4\pi r^2} \frac{dr}{dt} = \rho_{B(s)} \frac{dr}{dt} = k. \quad (5)$$

Separation of variables and integration between the indicated limits (*viz.* at time $t = 0$, $r = R$) yield

$$t = \frac{\rho_{B(s)}}{k} (R - r_c). \quad (6)$$

Let τ be the time for the particle to evaporate fully. Thus at $t = \tau$ we have $r = 0$, and from Eq. (6) we have

$$\tau = \frac{\rho_{B(s)} R}{k}. \quad (7)$$

Division of Eq. (6) by Eq. (7) thus yields an expression for the time fraction of the reaction in terms of radius, *viz.*

$$\frac{t}{\tau} = 1 - \frac{r}{R}. \quad (8)$$

The unreacted mass fraction $\alpha_{B(s)}$ is per definition given by

$$\alpha_{B(s)} = \frac{4/3\pi r^3 \rho}{4/3\pi R^3 \rho} = \frac{r^3}{R^3}. \quad (9)$$

It follows that

$$\frac{t}{\tau} = 1 - \alpha_{B(s)}^{1/3}. \quad (10)$$

This is similar in functional dependence to the shrinking sphere model given by Levenspiel [13] for the case of the chemical reaction controlled kinetics of a gas reacting with a solid. However, Eq. (10) uses residual mass fraction rather than the fraction of mass reacted. This is the form of the rate equation commonly found in engineering literature. Note that the left-hand side of Eq. (10) is a dimensionless time fraction. To transform Eq. (10) into the form more common to scientific literature, differentiation and substitution for τ are required to yield

$$\frac{d\alpha_{B(s)}}{dt} = -\frac{3k}{\rho_{B(s)} R} \alpha_{B(s)}^{2/3}. \quad (11)$$

This is the form given by Galwey and Brown [4] and Šesták [12]. However, density and particle size are not explicitly indicated in their formulation, and they use a single rate constant k' , as in Eq. (1). Comparison of Eqs. (1) and (11) shows that k' and k are related by

$$k = \frac{\rho_{B(s)} R k'}{3} \quad (12)$$

Note that the units of k' are s⁻¹, while those of k are kg m⁻² s⁻¹— as expected, since Eq. (1) represents the rate of change of a dimensionless quantity, while Eq. (4) represents a mass flux.

A similar treatment for a cylindrical particle, with the aspect ratio $D/L < 1$ (D being the diameter and L the length of the particle) yields

$$\frac{d\alpha_{B(s)}}{dt} = -\frac{2k}{\rho_{B(s)} R} \alpha_{B(s)}^{1/2}. \quad (13)$$

Comparison of Eqs. (11) and (12) with (1) clearly suggest that the average exponent of 0.54 determined from the n th-

Table 2
Literature kinetic data w.r.t. PTFE depolymerisation

Reference	Sample geometry/type	E_a (kJ mol ⁻¹)	k_0^* or k_0^{**}	n	Temperature range (°C)
[5]	Powdered	267–284	–	1	520–610
[6]	50–100 μm film, area unspecified	347	$3 \times 10^{19} \text{ s}^{-1*}$	1	360–510
[7]	Unspecified	318	10^{19} s^{-1*}	1	480–509
[8]	Unspecified	354	–	0	480–520
		191	–	0	520–570
[9]	Unspecified	316	$3 \times 10^{19} \text{ s}^{-1a*}$	1	Unspecified
[10]	3–5 μm	360–362	–	1	450–790
[11]	Unspecified, assumed powder	286	$6 \times 10^{19} \text{ s}^{-1*}$	0.71	450–650
		280	$3 \times 10^{16} \text{ s}^{-1*}$	0.02	
This work	800–1000 μm particulates	260 ± 20	$1.8 \times 10^{13} \text{ s}^{-1*}$ $8 \times 10^{12} \text{ kg m}^{-2} \text{ s}^{-1b**}$	0.54 ± 0.08	530–620

^a $\pm 4 \times 10^{19}$.

^b $\pm 2 \times 10^{12}$.

order approach is interpretable geometrically. The shape of the granules is used for this work falls midway between spherical and cylindrical, with coarse surfaces, and the exponent value between 1/2 and 2/3 is strong evidence that the empirical decomposition kinetics can be interpreted as supporting a standard shrinking particle model, with the rate directly proportional to the surface area of the residual mass.

Consideration of the data presented in Fig. 2 indicates that the greatest deviation from linearity occurs in the initial phase of the reaction. This can be interpreted as the particles losing their irregularity due to melting, and achieving a smoother surface and a more defined shape due to surface-tension effects. A rework from only the linear portion of the graphs in Fig. 2, unfortunately did not yield a tighter or more interpretable value for the reaction order. The average value becomes lower, but the standard deviation increases slightly. Shape changes during the melting are also expected due to softening and surface tension effects, and probably contributes to the large variance in the value of the reaction order.

Substituting the n th-order pre-exponential factor into Eqs. (11) and (13), and using the activation energy obtained from Fig. 3, the Arrhenius form of the rate constant in (4), (11) and (13) is

$$k = 8 \times 10^{12} e^{-260000/RT} \text{ kg m}^{-2} \text{ s}^{-1}. \quad (14)$$

The standard deviation of the pre-exponential factor k_0 is $= \pm 2 \times 10^{12} \text{ kg m}^{-2} \text{ s}^{-1}$.

2.4. Comparison with literature kinetic data

A selection of published kinetic parameters is listed in Table 2, and compared with the values generated in this study. As one would expect, there is fair correspondence amongst the values for the activation energy, and our value is firmly within the range quoted in the literature. There exists a difference of several orders of magnitude between our pre-exponential value and the literature values in general. Undoubtedly this can be attributed to non-homogeneous

heating, and to the fact that in our case the heating was not dominantly conductive.

Interestingly, in the case of Conesa and Font [11], who determined rather than assumed a reaction order, the value(s) thus obtained also suggest particle geometry and phase-boundary movement effects.

2.5. Conclusions

It is clear that sample geometry and non-homogeneous heating play a crucial role in interpreting the decomposition kinetics of PTFE. At least some of the inconsistencies and contradiction in the published data are attributable to this. The larger particle size used in this study is undoubtedly responsible for the fact that an interpretable exponent was obtained in our case. The majority of studies in the literature seem to refer to very finely divided samples in which homogeneous heating was obtained, and most often a reaction order was assumed rather than fitted. We have shown that certainly for coarser samples, geometric effects are important. For more complex geometries (*e.g.* where surface area and volume cannot be easily expressed in geometric parameters such as radius and extension) the rate law derived here, with which the moving boundary could be computed in larger heat-transfer models, becomes a temperature-dependent mass flux j from the surface, *i.e.*

$$\begin{aligned} -j(\mathbf{r}(t)) &= -\frac{1}{dA(\mathbf{r}(t))} \frac{dm_{B(s)}}{dt} = k \\ &= 8 \times 10^{12} e^{-260000/RT} \text{ kg m}^{-2} \text{ s}^{-1}. \end{aligned} \quad (15)$$

From our data, however, it is not possible to decouple heat transfer and chemical effects unambiguously, although the postulate that the rate limiting step in the movement of the outer phase boundary is controlled by chemical reaction rate rather than simple heat transfer, seems reasonable. Larger samples with well-defined geometries, which can be cross-sectioned to reveal thermal penetration depth during heating, would be needed for this. Work on this, and more detailed results of a microscopic study of the depolymerization process, will be reported at greater length.

3. Experimental

Isothermal TG analysis of unfilled PTFE *ex* Chemplast SA was performed using a PerkinElmer TGS2 TG analyser, with a Pt pan, working on a counterbalance principle. Single particles (800–1000 μm diameter) were introduced into the pan. This sample was heated to a predetermined temperature at a heating rate of $40\text{ }^{\circ}\text{C min}^{-1}$ with nitrogen as a carrier gas, at a flow of 30 ml min^{-1} , and then maintained at constant temperature for 40 min. Temperature measurement on this instrument was done at the bottom of the platinum pan.

Acknowledgements

The authors would like to thank NECSA's Messrs Danie Moolman and B.M. Vilakazi for performing the thermogravimetric analyses, and Dr. Kobus Wagenaar and Dr. Andries 'Cassie' Carstens for extremely useful discussions.

References

- [1] E.E. Lewis, M.A. Naylor, *J. Am. Chem. Soc.* 69 (1947) 1968–1970.
- [2] I.J. Van der Walt, O.S.L. Bruinsma, *J. Appl. Pol. Sci.* 102 (2006) 2752–2759.
- [3] E. Meissner, A. Wróblewska, E. Milchert, *Polym. Degrad. Stab.* 83 (2004) 163–172.
- [4] A.K. Galwey, M.E. Brown, *Thermal Decomposition of Ionic Solids*, Elsevier Science, Amsterdam, 1999, pp. 102–105.
- [5] C.D. Doyle, *J. Appl. Polym. Sci.* 5 (15) (1961) 285–292.
- [6] J.C. Siegle, L.T. Muus, T.-P. Lin, H.A. Larsen, *J. Polym. Sci. A 2* (1964) 391–404.
- [7] J.M. Cox, B.A. Wright, W.W. Wright, *J. Appl. Polym. Sci.* 8 (1964) 2935–2950.
- [8] B. Carroll, E.P. Manche, *J. Appl. Polym. Sci.* 9 (1965) 1895–1903.
- [9] B. Holzknrecht, *Int. J. Heat Mass Transfer* 20 (1977) 661–668.
- [10] S. Morisaki, *Thermochim. Acta* 25 (1978) 171–183.
- [11] J.A. Conesa, R. Font, *Polym. Eng. Sci.* 41 (12) (2001) 2137–2147.
- [12] J. Šesták, *Thermochim. Acta* 3 (1971) 1–12.
- [13] O. Levenspiel, *Chemical Reaction Engineering*, John Wiley & Sons, New York, 2006.